phys. stat. sol. (c) **5**, No. 6, 2092–2095 (2008) / **DOI** 10.1002/pssc.200778446

physica status solidi c
www.pss-c.com
current topics in solid state physics

Growth of nonpolar cubic GaN/AlN multiple quantum wells with intersubband transitions for 1.5 μm applications

D. J. As[*,1], J. Schörmann[1], E. Tschumak[1], K. Lischka[1], E. A. DeCuir[2], and M. O. Manasreh[2]

[1] Department of Physics, University of Paderborn, Warburger Str. 100, 33095 Paderborn, Germany
[2] Department of Electrical Engineering, University of Arkansas, 3217 Bell Engineering Center, Fayetteville, Arkansas 72701, USA

Received 3 September 2007, revised 8 January 2008, accepted 12 January 2008
Published online 25 March 2008

PACS 61.05.cp, 61.05.jh, 78.30.Fs, 78.66.Fd, 78.67.Pt, 81.15.Hi

[*] Corresponding author: e-mail d.as@uni-paderborn.de, Phone: +49 5251 60 5838, Fax: +49 5251 60 5843

Cubic GaN/AlN short-period multiple quantum well structures were grown at 720 °C by plasma-assisted molecular beam epitaxy on free standing 3C-SiC substrates. The samples consist of 100 nm thick GaN buffer and 20 periods of GaN/AlN active regions. The thickness of the AlN barrier is 1.35 nm for all samples, while the thickness of the GaN well varies between 1.6 nm-2.10 nm depending on the samples. The periodicity of the GaN/AlN active regions was confirmed by the presence of several peaks in the high resolution x-ray diffraction (HRXRD) spectra. The thickness of the total period was estimated by fitting the HRXRD data using a dynamic scattering theory. Room temperature measurements of the optical absorption spectra of the intersubband transitions were obtained using a Bruker IFS-125HR spectrometer. The peak position wavelengths of these transitions were observed in the spectral region of 1.5–2.0 μm and confirmed theoretically by using a self-consistent Poisson-Schrödinger model.

1 Introduction Intersubband transitions (ISBT) form the basis for quantum well infrared photodetectors (QWIP) and Quantum cascade lasers (QCL) [1]. Due to the wide band gaps and the large band offsets between AlN and GaN this group of III-Nitrides offer intersubband transitions in the technologically important infrared 1.3-1.5 μm spectral range [2-6]. Nevertheless, a major challenge for the design of GaN/AlN devices based on ISBT is the presence of strong intrinsic piezoelectric and pyroelectric fields generated by sheet charges at each hetero-interface [7]. Efforts to circumvent these large built-in electrostatic fields have been accomplished by using nonpolar hexagonal structures [1] or by using cubic zincblende structures [8]. The growth of nonpolar cubic GaN/AlN multiple quantum well (MQW) structures on (001) oriented substrates will eliminate the detrimental strong spontaneous polarization fields [9], allowing easier design of the complex MQW structures with various quantum well widths as it is necessary for QCL systems.

2 Experimental All quantum structures were grown at 720 °C on free standing 3C-SiC (001) substrates by plasma assisted molecular beam epitaxy (MBE). A 100 nm thick cubic GaN (c-GaN) buffer layer was deposited on a 3C-SiC substrate using the Reflection High Energy Electron Diffraction (RHEED) control of the growth process as described in reference [10]. Subsequently, a 20 period GaN/AlN superlattice (SL) was grown. The barrier thickness was fixed at 1.35 nm for all samples while the well thickness is changed for different samples, but kept in the range of 1.6-2.1 nm. Finally the quantum structures were capped with a 100 nm thick c-GaN layer. After each layer the growth was interrupted for 20 seconds to allow excess metal to evaporate from the surface. Three different SL samples with different quantum well widths were used in this study and waveguides were cut from each sample.

A high resolution x-ray diffractometer (HRXRD) was used to characterize the structural properties and the diffraction profiles of our AlN/GaN superlattices samples. The Diffraction profiles were analyzed by using a dynamic diffraction model which provides the mean superlattice pe-

riod with a high precision, better than 0.1 nm. However it does not directly provide the thickness of barrier and well and does not take into account thickness fluctuations [11].

The background doping of a GaN reference layer was measured by electrochemical capacitance-voltage profiler giving a bulk carrier concentration (N_{3D}) on the order of $1.33x10^{18}cm^{-3}$ [8]. This doping yields a Fermi energy level above the ground state energy level, which is a necessary condition for the observation of intersubband absorption.

The optical absorption measurements were recorded using a Bruker Fourier-transform 125HR spectrometer. The interferometer configuration consists of a quartz-halogen light source, an InSb cooled detector, and a calcium fluoride beam-splitter. This configuration permits the measurements in the spectral range of 1-3 μm. The light used in this experiment was unpolarized in nature, however, a waveguide geometry was used to provide a polarization component normal to the growth direction. This geometry was necessary to satisfy selection rules in QWs and enable electron-photon coupling. The waveguide provides multiple passes, i.e., this increases the aborption length, thereby increasing the relative absorption in these superlattices.

A self-consistent Poisson Schrödinger model (1D-Poisson) is used to calculate the bound state energy levels as a function of the well and barrier widths from which the energy difference between the ground and first excited states were obtained [12]. These calculated values are then compared to the peak position energies obtained from the optical absorption spectra of the intersubband transitions.

3 Results and discussion One of the key-issues for a structurally perfect superlattice is the carefully control of the growth in the MBE reactor using in-situ RHEED. Recent investigations showed that optimum growth conditions of c-GaN were found when an one monolayer (ML) Ga coverage is formed at the surface [10]. A typical RHEED time scan during the growth of an AlN/GaN superlattice is shown in Fig. 1. The shaded area indicates the growth of the individual layers. Clear RHEED-oscillations of c-AlN were seen during the growth of the AlN barrier material revealing a growth rate of 0.11 ML/s. For the cubic GaN RHEED-oscillations - and therefore in-situ growth rate measurement - were suppressed due to the one ML Ga-coverage, which is necessary for a smooth growth surface. The growth rate under this Ga-rich condition was estimated to be 0.26 ML/s with post growth thickness measurements. All time scans are identical, revealing a highly reproducible growth process of the quantum wells. The structural properties were measured by a high resolution x-ray diffraction technique. Figure 2 shows the ω-2Θ scan of the (002) reflex of a 20 periods GaN/AlN superlattice structure (upper curve). A periodicity of 3.1 nm was estimated from the difference of the superlattice peaks by using a dynamic simulation program (curve labelled simulation in Fig. 2). With the knowledge of the growth rates of AlN obtained from RHEED oscillations, a AlN barrier and a GaN well width of 1.35 and 1.75 nm were determined, respectively. Reciprocal space mapping (RSM) of the asymmetric GaN (-1-13) reflex show that for all our samples the AlN barriers are pseudomorph to the c-GaN buffer.

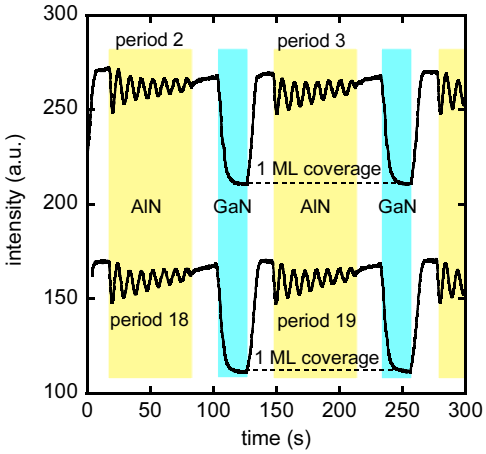

Figure 1 RHEED intensity time scans measured during the growth of quantum well number 2, 3, 18 and 19 of a 20-fold cubic GaN/AlN short period superlattice.

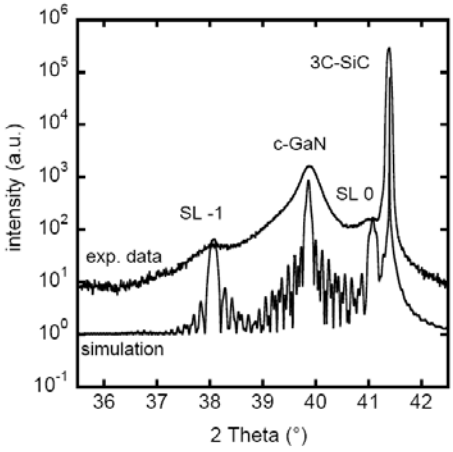

Figure 2 HRXRD ω–2Θ spectra obtained for a 20 period of 1.75nm GaN/ 1.35 nm AlN sample.

The surface roughness of these structures was investigated by atomic force measurements (AFM). The RMS roughness on a 5x5 μm^2 scan area is typically about 2.6 nm, which is in the order of the best values reported for bulk c-GaN [10].

The room temperature absorbance spectra of the intersubband transition in three superlattice samples are plotted in Fig. 3. The absorbance is defined as the product of the absorption coefficient (α) and the total thickness of the quantum wells in the superlattice (L). In these coupled wells, splitting of the energy levels occur due to overlap between localized wave functions in neighbouring quantum wells, which leads to the formation of mini-bands. The full width at half maximum (FWHM) of each absorption

peak varies between 180 to 220 meV. Notably the absorbance peak of sample C is close to the wavelength of 1.55 µm, which is of relevance for the application of c-GaN/AlN SLs for optical communication light detectors. While the shape of the spectra of sample B and C is close to a single Lorentzian, the best fit of the absorption spectrum of sample A has been obtained by two Lorentzians with peak wavelength at 2.1 µm and 1.87 µm (dashed curves), respectively. The FWHM of the individual fits is ~ 90 meV, which is comparable to linewidths observed in hexagonal AlN/GaN SLs [13].

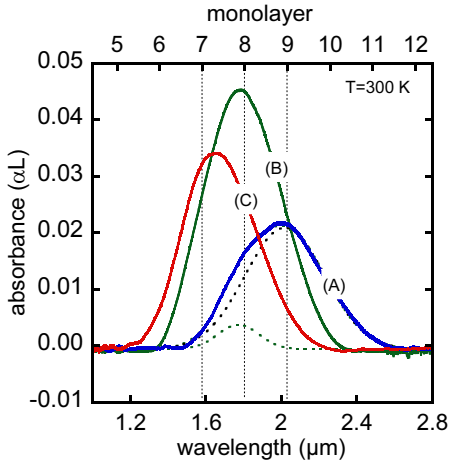

Figure 3 Room temperature absorbance spectra of three intersubband transitions measured for cubic GaN/AlN superlattice samples with different well thicknesses.

Figure 4 shows the transition energy between the ground state E_0 and E_1 of the GaN/AlN SLs vs. the GaN well width given in nm and GaN-monolayers. The solid line is calculated using a self-consistent Poisson Schrödinger model [12]. We used an electron effective mass of $0.19m_0$, where m_o is the free electron mass. An important parameter which is incorporated in these calculation is the ratio between the conduction and valence band offsets (ΔE_{CV}). It was found that the best agreement between the experimental data and calculated results shown in Fig. 4 is when $\Delta E_{CV} = 70{:}30$.

The solid squares indicate the peak energy of the experimental absorption spectra of sample A, B and C. Notably, the well width of sample B and C, which have a single line absorption spectrum are close to an integer number of monolayers. The dots are the peak energies of the fitted curves of spectrum A. They correspond to well width of 8 and 9 monolayers, which indicate a well thickness fluctuation of one monolayer in this sample.

4 Conclusion Nonpolar cubic AlN/GaN superlattices with intersubband transition near the technological important 1.55 µm spectral region were grown by plasma assisted MBE. The periodicity of the AlN/GaN active regions was confirmed by HRXRD. Room temperature absorption measurements showed ISBTs in the spectral region of 1.5-2.0 µm which were theoretically confirmed by using a self-consistent Poisson-Schrödinger model. Lorentzian peaks with linewidths of ~ 90 meV were observed within the intersubband absorption spectra, and were attributed to monolayer fluctuations of the QW width.

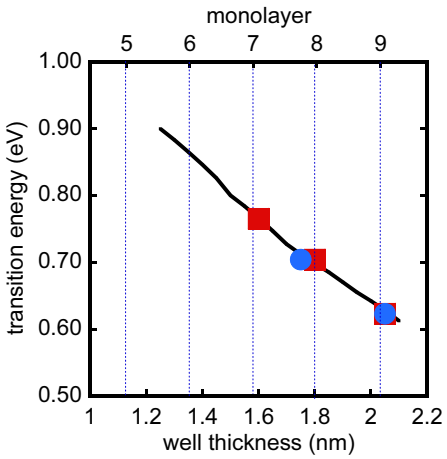

Figure 4 Calculated intersubband transition energy (full line) and measured peak position energies (symbols) vs. well width of cubic GaN/AlN superlattices.

Acknowledgements The authors thank H. Nagasawa and M. Abe from SiC Development Center, HOYA Corporation, Japan, for supplying the 3C-SiC substrates. The work at the University of Arkansas was funded by the Air Force Office of Scientific Research (programm manager: Gernot Pomerenke) and by the Arkansas Science & Technology Authority.

References

[1] G. Gmachl and H.M. Ng, Electron. Lett. **39**, 567 (2003).
[2] K. Kishino, A. Kikuchi, H. Kanazawa, and T. Tachibana, phys. stat. sol. (a) **192**, 124 (2002).
[3] N. Iizuki, K. Kaneko, and N. Suzuki, Appl. Phys. Lett. **81**, 1803 (2002).
[4] G. Gmachl, H.M. Ng, S.-N.G. Chu, and A.Y. Cho, Appl. Phys. Lett. **77**, 3722 (2000).
[5] D. Hofstetter, S.-S. Schad, H. Wu, W. J. Schaff, and L. F. Eastman, Appl. Phys. Lett. **83**, 572 (2003).
[6] E. A. DeCuir, Jr., E. Fred, B. S. Passmore, A. Muddasani, M. O. Manasreh, J. Xie, H. Morkoc, M. E. Ware, and G. J. Salamo, Appl. Phys. Lett. **89**, 1 (2006).
[7] F. Bernardini, V. Fiorentini, and D. Vandenbuilt, Phys. Rev. B **56**, R10024 (1997).
[8] E. A. DeCuir, Jr., E. Fred, M. O. Manasreh, J. Schörmann, D. J. As, and K. Lischka, Appl. Phys. Lett. **91**, 041911 (2007).
[9] J. Schörmann, S. Potthast, D. J. As, and K. Lischka, Appl. Phys. Lett. **89**, 131910 (2006).
[10] J. Schörmann, S. Potthast, D.J. As, and K. Lischka, Appl. Phys. Lett. **90**, 041918 (2007).

[11] D. Bowen and B. Tanner, High Resolution Diffractometer and Topography (Taylor & Francis Ltd., New York, 1998).
[12] I. H. Tan, G. L. Snider, L. D. Chang, and E. L. Hu, J. Appl. Phys. **68**, 4071 (1990).
[13] M. Tchernycheva, L. Nevou, L. Doyennette, F. H. Julien, E. Warde, F. Guillot, E. Monroy, E. Bellet-Amalric, T. Remmele, and M. Albrecht, Phys. Rev. B **73**, 125347 (2006).